Structural Performance of Parallel Concrete Panel Container Towards Green Coastal and Port's Retaining Wall: A Comparison of Tie Rod Configurations

Hamid, Affandy
National Research and Innovation Agency, Center for Hydrodynamics Technology

Suranto
National Research and Innovation Agency, Center for Hydrodynamics Technology

Dinar C. Istiyanto
National Research and Innovation Agency, Center for Hydrodynamics Technology

Rizaldi C. Yuniardi
National Research and Innovation Agency, Center for Hydrodynamics Technology

他

https://doi.org/10.5109/7236917

Structural Performance of Parallel Concrete Panel Container Towards Green Coastal and Port's Retaining Wall: A Comparison of Tie Rod Configurations

Affandy Hamid, Suranto, Dinar C. Istiyanto, Rizaldi C. Yuniardi,
Shafan A. Aziiz, Yofan T.D. Harita, Aloysius B. Widagdo, Syahrizal A. Latief,
Ika Wulandari, Raka Firmansyah*

National Research and Innovation Agency, Center for Hydrodynamics Technology, Indonesia

*Author to whom correspondence should be addressed:
E-mail: affa002@brin.go.id

Abstract: A retaining wall is among the common structures required in the coastal and port areas. This structure is constructed to support and protect elevated land near the coastline, e.g., coastal road embankments, or to develop port service areas, such as container yards, loading-unloading areas, etc. Despite its limited actual field implementation, a Parallel Concrete Panel Container type of wall structure is available. It has been promoted for its ease of construction in the coastal area, less use of concrete material, and less space occupation. The present study assessed the potential implementation of this structure as a retaining wall in coastal and port areas. In this study, the structural stability and strength analysis of the PCP is carried out for two types of tie rod configurations. The analysis was conducted using the numerical simulation software of PLAXIS 2D and SAP 2000. The results show that the container with a diagonal bonding configuration type A performs better overall structural efficiency than the one with a horizontal bonding configuration type B. The PLAXIS modeling results showed that PCP types A and B had safety factor values of 1.35 and 1.32, respectively. These values indicated that both structures worked stably. Additionally, it implies that the soil has sufficient strength to support the applied loads without failure.

Keywords: Retaining Wall; Parallel Concrete Panel; Structural Stability

1. Introduction

Coastal regions have a lot of potential for development into high-value industries like ports, tourism, and residential areas, such as Indonesia, which has an 81,000 km shoreline[1]. However, climate change has made this region increasingly vulnerable to wave erosion, storm surges, and inundation caused by rising sea levels and tidal fluctuations. In Indonesia's northern coastal areas of Java, particularly in Jakarta, Semarang, and Demak, shoreline issues are prevalent and have been the subject of several studies. Projections indicate a potential increase in water level of approximately 1.8 meters and a 37% rise in the spatial inundation area around Jakarta's shoreline[2]. Demak has experienced significant shoreline abrasion, with an average coastline change of -119.08 meters, due to sea level rise and land subsidence[3]. Jakarta and Semarang also face subsidence rates ranging from 3 to 10 cm per year, resulting in coastal inundation, flooding, and infrastructure damage[4].

To enhance the sustainability performance of port and coastal infrastructure, it is essential to identify all pertinent aspects of sustainability, define appropriate performance metrics, utilize quantification tools, and propose necessary intervention measures[5]. An approach can be taken by providing coastal protection infrastructure to overcome and prevent damage to this area. Generally, several types of coastal protection structures have been built, such as seawalls, sea dikes, revetments, breakwaters, and groins. Infrastructure is crucial in protecting and providing facilities to protect the environment and humans[6]. Currently, infrastructure provision is approached with a green infrastructure approach, which is the key to achieving sustainability[7]. Green infrastructure systems offer a framework for future growth that fosters various ecological, social, and economic benefits, which aid in preserving and restoring naturally functioning ecosystems[8]. The construction sector is mainly responsible for the consumption of natural resources and the pollution of the environment. This is why eco-friendly and innovative buildings result from sustainable environmental policies[9]. In designing marine building structures, it is also crucial to consider safety concerns that pertain to the structure's lifetime. The

longevity of each form of construction varies based on the building's function, the environmental pressure it experiences, and the conditions of the soil on the seabed[10].

Coastal Engineering Manual[11] categorizes coastal structures into two primary types: sloping-front and vertical-front constructions. Sloping-front structures mostly consist of rubble-mound constructions reinforced with rock or concrete armor sections. Vertical-front structures are mostly made from sand-filled concrete caissons or enormous concrete blocks on rubble stone bedding. Due to cost considerations and environmental impact[12], concrete caissons are frequently positioned on a raised mound of quarry rock in deep water. A vertical-front structure has advantages over sloping rubble-mound structures in terms of its reduced reliance on natural rock material and its flexibility to be customized for ship berthing and mooring[13]One advantage of vertical-front structures is that they use fewer natural rocks, keeping natural resources sustainable. However, a vertical caisson structure necessitates substantial concrete, downgrading its economic feasibility.

Various designs of concrete-made vertical-front structures are available and suited for specific environments. Recently, a patented design called Parallel Concrete Panel (PCP) Container was introduced as an eco-friendly innovation alternative for shoreline building[14]. The structure has been patented under patent numbers IDP000019181 and IDP0000071957[15].

The PCP, as precast concrete, offers significant technical advantages over conventional reinforced concrete structures[16]. The structure can eliminate the requirement for piles and pile caps, which are needed to support conventional structures to retain soil. This advantage brings cost efficiency through all of the construction stages and the use of materials[17]. The PCP also has the potential to be a more environmentally friendly structure due to the small volume of concrete material and the use of fill material from a suitable local environment. This structure has been broadly applied to land and river structures but has not been used as a coastal protection structure. The work demonstration of the installed structure shows a good and stable result[17]. Therefore, we further explore the structural behavior of PCP as shoreline protection in this study, specifically for a coastal retaining wall.

2. Composition of a PCP Container

This structure is a soil container system consisting of three elements. The first element is a pair of concrete panels with pre-plated solidity (1), the second element is the tie rods of steel (2), and the third element is filling materials (3). These elements are bound to each other with all the geometry of its attaching system. The parallel panels are set up at the designed distance and bound by a series of tie rods to form a three-dimensional container box that becomes self-stable after it is filled with filling

material. The box width in these three dimensions is calculated based on the loads that work on the containers. Once the PCP container box is filled and solid with filler material, it will stand against any vertical or horizontal pressure forces. The tie rods will work against any tensile forces due to the outward loads on the parallel panels. The series of containers can develop or grow in vertical and horizontal/length directions.

The PCP may be considered a back-to-back mechanically stabilized earth (BBMSE) wall by its structural form, as is described and demonstrated in the FHWA design guidelines[18]. It can sustain significant loadings and deformations due to the interaction between the backfill material and the reinforcement elements[19]. It is also known that an MSE structure can be constructed with a leveling pad to support the facing panels, except in the case of highly compressible clayey soil or soft clays[20]. Previous study[21] Recommends an optimum ratio of the reinforcement overlap (i.e., the distance between walls and the total height of the walls) at 0.3H to get an efficient magnitude of tensile works in the reinforcement material (rods or geogrid).

3. Structural Analysis and Modelling Methods

Two models will be examined in this study. Two variations of tie rod configurations between concrete panels are used in retaining walls to observe the structure's behavior under applied loads. The concrete properties in this modeling conform to marine environment standards[22]. The two model configurations are as follows:

1. Parallel concrete panel with diagonal tie rod configuration (Type A) and

2. Parallel concrete panel with horizontal tie rod configuration (Type B).

Type A refers to the original patented shape with a diagonal tie rod configuration. Type B is an alternative tie rod configuration that considers the requirement for smaller tie rods. This study analyzes the optimum tie rod size that provides excellent structural stability for the specified concrete panel size. Figures of concrete panels with a diagonal tie rod configuration (Type A) and a horizontal tie rod configuration (Type B) are shown in Fig. 1 and 2, and the cross sections for Type A and Type B are shown in Fig. 3 and 4, respectively.

Software SAP2000 v.21 and PLAXIS 2D are used for structural modeling. The loads acting on the structure refer to design standards, manuals, and guides, including references[23] [24]. The utilization of SAP2000 for analysis reduces the complexity of the process, such as the extensive manual involvement and the complex iterative process required to determine the optimal parameters, compared to the laborious manual design process[25]. Additionally, the PLAXIS software can conduct static and dynamic analyses[26]. This study will use both analytical tools to offer a comprehensive assessment of the structural
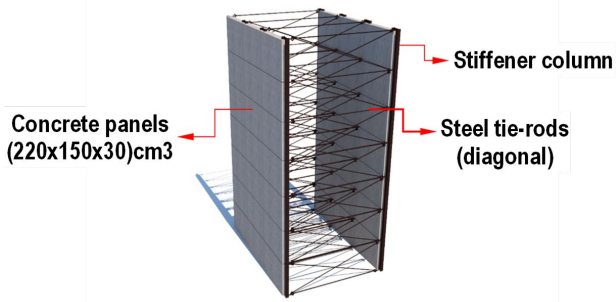
integrity and capacity of the foundation.

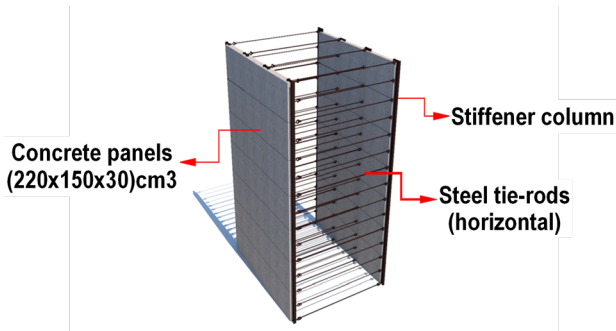**Fig. 1:** Parallel concrete panel with diagonal tie rod configuration (Type A)

Fig. 2: Parallel concrete panel with horizontal tie rod configuration (Type B)
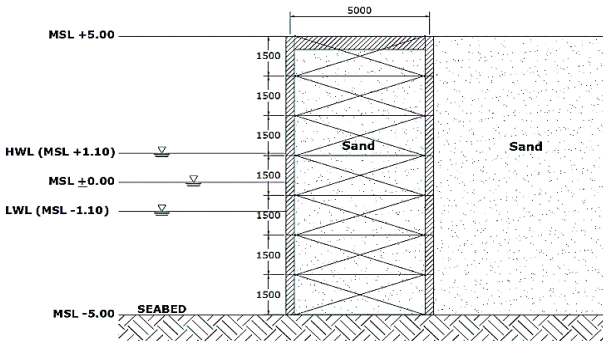

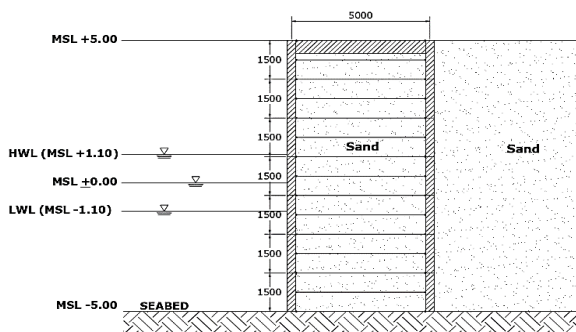**Fig. 3:** Parallel concrete panel cross-section with diagonal tie rod configuration (Type A)

Fig. 4: Parallel concrete panel cross-section with horizontal tie rod configuration (Type B)

3.1. Load Calculation for Structural Analysis

Due to the daily exposure of the structures to waves[27], the wave load is calculated using wave modeling data that has a 100-year return period[28], with a significant wave height (Hs) of 2.93 meters and a wave period (T) of 12.53 seconds. Table 1 shows all working load descriptions.

Table 1. Load Descriptions

Live load (Vehicle distribution load)	
Elevation +5.50 MSL	P= 418.42 kg m^{-2}
Elevation -5.00 MSL	P= 418.42 kg m^{-2}
Water level	P= 0 kg m^{-2}
Elevation -5.00 MSL	P= 6253 kg m^{-2}
Elevation -5.00 MSL	P= 5000 kg m^{-2}
Wave load; Goda (1973)[29] dan Takahashi (1994)[30]	
Elevation +5.50 MSL	P$_1$= 2324.296 kg m^{-2}
Elevation +1.10 MSL	P$_2$= 5353.396 kg m^{-2}
Elevation -5.00 MSL	P$_4$= 4940.181 kg m^{-2}
Filler load *(Rankine Theory of earth pressure* (1857))[31]	
Elevation +5.50 MSL	P= 0 kg m^{-2}
Elevation +1.10 MSL	P= 1950.81 kg m^{-2}
Elevation -5.00 MSL	P= 9548.28 kg m^{-2}
Earthquake load (Indonesian earthquake spectrum 2021)[32]	
0,2S Spectral Acceleration	Ss = 0.4293 e
0,1S Spectral Acceleration	S1 = 0.1291 g
Peak Ground Acceleration	PGA = 0.20 g
Risk category	III
Earthquake Importance Factor	Ie =1.25
Response modification coefficient	R = 6
Earthquake factor	g.I$_e$/R = 2.044

3.2. Load Distribution

Based on the load calculation analysis results, Figure 5 displays the load distribution graphics for the live load, hydrostatic load, wave load, and fill material load based on the findings of the load calculation investigation.
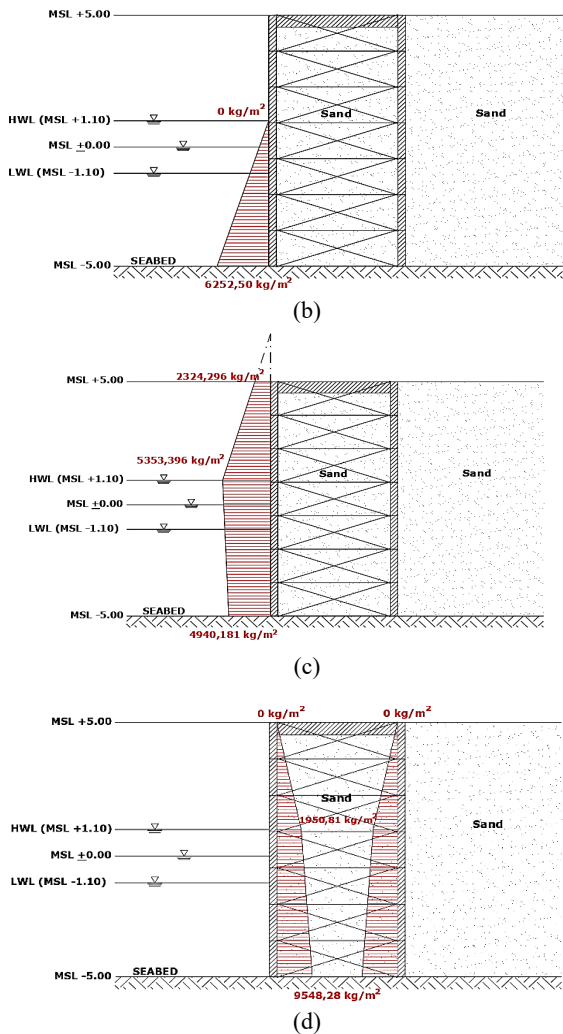

(a)
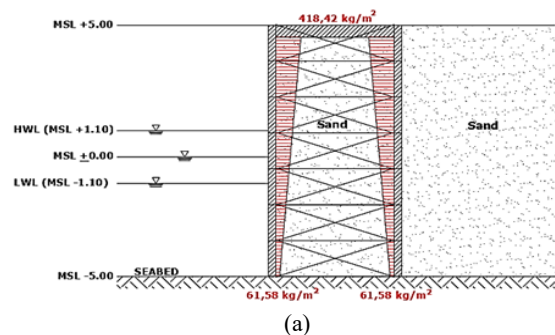
Fig. 5: (a) Live load distribution (b) Hydrostatic load distribution. (c) Wave load distribution. (d) Fill material load distribution.

3.3. Load Combination

Table 2 lists the load combinations used in the SAP2000 structure analysis modeling to determine the structure's maximum capacity. Regarding basic combinations of loads, SNI 1727:2020 section 2.3.2 is referred to in this load combination[33].

Table 2. Load Combination

Combination	Load Combination
Comb 1	1.4D
Comb 2	1.D + 1.6L
Comb 3	1.2D + 1.6L + 1.6H + 1.2F
Comb 4	1.4D + 1.4W +1.6H + 1.4F
Comb 5	1.2D + 1L + 1.2W + 1.6H + 1.2F
Comb 6	1.2D + 1L + 1EX + 0.3EY + 1.6H + 1.2F
Comb 7	1.2D + 1L + 1EY + 0,3EX + 1.6H + 1.2F
Comb 8	0.9D + 1EY + 0.3EX + 0.9W + 1.6H + 0.9F

Where,

D	: Dead load
L	: Live load (vehicle load)
H	: Filling material load
F	: Hydrostatic load
W	: Wave load
EX	: Earthquake load in x direction
EY	: Earthquake load in y direction

3.4. Material for Foundation Interaction Modeling

Specific descriptions of soil, tie rod, and concrete panel properties are required to simulate foundation interaction using PLAXIS-2D. In the present study, sand base soil with a dense consistency is designed for the foundation soil material and the structure's filling material (space between parallel panels). However, since there is a design requirement that the subgrade of the foundation must be impermeable, the permeability parameter is set up at least at 0.00864 m/day (1x10-6 cm/second) in SNI 8460-2017 concerning Geotechnical Design Provisions[34]. Further, the tie rods are designed as anchors, and the panels are considered concrete plates in the model. The PLAXIS modeling takes into account the impact of seismic load. A study has reported that the average Peak Ground Acceleration (PGA) in the Jakarta area reaches 1.0 g, or there is a 2% chance of exceeding this value within 50 years[35].

The following tables summarize soil, tie rod, and concrete panel parameters adopted for the present modelling input.

Table 3. Soil parameters

Soil Parameter	Units	Soil Base	Filling Soil Material
γ_{unsat}	kN m^{-3}	19	19
γ_{sat}	kN m^{-3}	21	21
E_{50}^{reff}	kN m^{-2}	50000	50000
E_{oed}^{reff}	kN m^{-2}	50000	50000
E_{ur}^{reff}	kN m^{-2}	150000	150000
ν	-	0.2	0.2
c'	kN m^{-2}	1	1
φ	º	40	40
Ψ	º	0	0
k_x, k_y	m/day	0.00864	8.64

Table 4. Tie Rod Parameters.

Anchor Parameter	Unit	Tie Rods
EA	kN	10.31x10^4
$L_{spacing}$	m	1

Table 5. Concrete panel parameters.

Plate Parameter	Unit	Panel	Covering Material
EA	kN m^{-1}	8.124x10^6	16.25x10^6
EI	kN m^{-2} m	60.93x10^3	48.75x10^4
d	m	0.3	0.6
w	kN m^{-1} m	6.828	13.66
ν	-	0.2	0.2

Where,

E_{50}^{reff}	:	Soil stiffness value based on a triaxial test (CD) with stress value (Preff) = 100 kPa[36].
E_{oed}^{reff}	:	The soil stiffness value is based on the oedometer test.
E_{ur}^{reff}	:	Soil stiffness value in loaded and unloaded conditions (around 2 to 5 times of E_{50}^{reff}), but the Plaxis used is three times the E_{50}^{reff} [36].
m	:	strength to pressure level dependence (Oedometer test)
v_{ur}	:	*Poisson ratio.*
Υ_{dry}	:	Dry weight of soil (N m^{-2}).
Υ_{sat}	:	The specific weight of saturated soil (kN m^{-2}).
c	:	cohesion (kN m^{-2})
$\emptyset$	:	shear angle (^{0})
k_x	:	Horizontal soil permeability coefficient (m day^{-1}).
k_y	:	Vertical soil permeability coefficient (m day^{-1}).

The stiffness value of loaded and unloaded soil (E_{ur}^{reff}) is obtained based on a value determination of 3 times the E_{50}^{reff} [36].

4. Modelling Result and Discussion

Elaboration on the configuration of the tie rod is considered necessary because of its vital role in the whole structure's integrity. It is expected to assume that the smaller the diameter of the tie rod, the more economical the construction is. This study would like to investigate the configuration that requires a smaller tie rod diameter under the same load and with the same concrete panel size. The calculation work was carried out using SAP2000 software to obtain the final size of tie rod diameters as well as the maximum moment capacity of the concrete panel.

The SAP2000 algorithm uses the Unit Check Ratio value (UCR) to indicate the optimum integral capacity of the structure. The UCR equals 1, which means the maximum limit capacity of the structure.

Figure 6 and Figure 7 shows the graphic presentation of the modeled PCP structure configuration (SAP2000) and the analysis results for diagonal tie rod configuration (Type A) and horizontal tie rod configuration (Type B), respectively. Table 6 summarizes the modeling results for two tie rod configuration variants, showing the tie rod's related optimum diameter, the corresponding Unit Check Ratio (UCR) value, and the maximum moment value associated with the concrete panel.
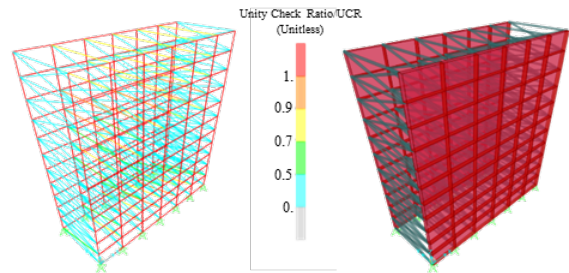

Fig. 6: Graphic presentation of the structural model configuration (SAP2000) and the analysis results for parallel concrete panel with diagonal tie rod configuration (Type A)
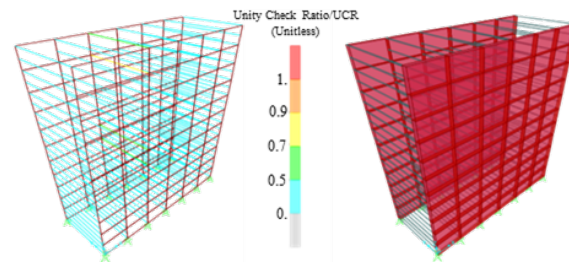

Fig. 7: Graphic presentation of the structural model configuration (SAP2000) and the analysis results for parallel concrete panel with horizontal tie rod configuration (Type B)

The modeling results in Table 6 indicate that Type B, featuring a horizontal tie rod configuration, necessitates a smaller rod diameter than Type A, which adopts a diagonal tie rod configuration. However, despite the reduced rod diameter, Type B exhibits a considerably higher maximum moment within the concrete panels. This underscores the direct correlation between tie rod configuration and its diameter on the resultant structural behavior, providing valuable insights for structural design optimization.

Table 6. Modeling Results of Parallel Concrete Panel Structure with Variation of Tie Rod

Tie Rod Configuration	Optimum Tie Rod Diameter	Max UCR	Max Moment Concrete Panel
text	*mm*	*unitless*	*ton-m m^{-1}*
Type A	140	0.984	1.571
Type B	90	0.827	79.008

Type A: diagonal tie rod configuration; Type B: horizontal tie rod configuration.

In the above consideration, an additional model of tie rod configuration, called Type C, was investigated. This

Type C has the same tie rod configuration as Type A, but its horizontal tie rod diameter is smaller than its diagonal counterparts. The modeling results show that the reduction of horizontal tie rod diameter in this configuration still maintains the optimum integral capacity of the structure while efficiently keeping the maximum moment in the concrete panel. This implies that this combination of horizontal and diagonal tie rods proves more economically advantageous considering the tie rod diameter specifications. The results of this Type C modeling exploration are presented in Table 7 for further comprehensive examination and reference.

Table 7**.** Modeling Results of Parallel Concrete Panel Structure with Combination of Tie Rod Configurations (Horizontal and Diagonal)

Tie Rod Configuration	Optimum Tie Rod Diameter		Max UCR	Max Moment Concrete Panel
text	Horizontal mm	Diagonal mm	unitless	ton-m m^{-1}
Type C*	25	140	0.959	1.881

** Type C equals type A but has a smaller horizontal tie rod diameter.*

Concurrently, the interaction between the structural component and its foundation is modeled using the Plaxis 2D software, with the resultant output including critical parameters like the safety factor and displacement. Safety factor analysis is needed to ensure the global stability of structures and soil structures. The analysis results are presented in Table 8, encompassing the parallel concrete panel Type A and Type B structures. Figures 8 and 9 show a graphic presentation of soil displacement under load conditions on Plaxis 2D for Type A and Type B of parallel concrete panels, respectively.

Table 8**.** Modeling Results of PCP Structures with Variation of Tie Rod Configurations on Plaxis 2D.

Tie Rod Configuration	Stability	Safety Factor	Displacement	
			X direction	Y direction
text	text	-	m	m
Type A	Stable	1.35	-0.1157	-0.2749
Type B	Stable	1.32	-0.0992	-0.2751

Type A: diagonal tie rod configuration; Type B: horizontal tie rod configuration.
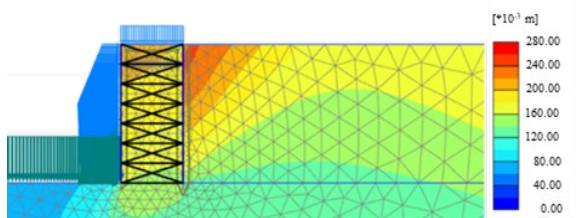
Total displacements |u| (scales up 10.0 times)
Maximum value = 0.2749 m (Element 362 at Node 4070)
Fig. 8: Numerical simulation of total displacement due to total load on PCP Type A
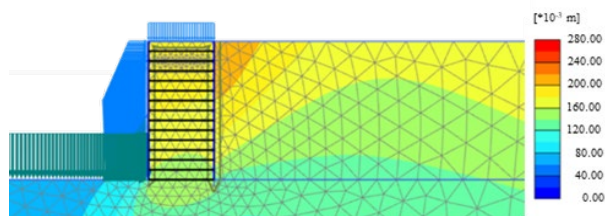
Total displacements |u| (scales up 10.0 times)
Maximum value = 0.2751 m (Element 362 at Node 4070)
Fig. 9: Numerical simulation of total displacement due to total load on PCP Type B

The modeling results reveal a need for a more substantial disparity between the structural behaviors of Type A and Type B configurations. However, Type A demonstrates slightly heightened stability with a safety rating of 1.35 compared to Type B with a safety rating of 1.32. These SFs of both types fulfill the bottom limit specifications outlined in SNI 8460:2017[34], which stipulates that the minimum safety factor mandated for analyses utilizing a pseudo-static model under seismic loading conditions exceeds 1.1 (SF > 1.1). This means the present concrete panel wall configurations are stable even without supporting systems, e.g., pile foundations. Hulagabali et al[20]. A similar type of retaining wall was studied, and it was concluded that in most cases, the construction of a segmental precast concrete panel wall does not urgently require a foundation. It can be constructed with a leveling pad to support the facing panels, except for highly compressible clayey soil or soft clays.

According to a similar study by Lajevardi et al[37], the safety factor obtained can vary depending on the type of reinforcement used and the design factor between the width and height structure ratio. Compared to this study, Lajevardy obtained a higher safety factor value of around 1.33-2.28 using three reinforcement types: steel strips and geosynthetics (GS50 and GS HS). In addition, the study indicated that as the distance between walls becomes

closer, the wall stability increases.

Considering displacement, there is virtually no discernible distinction between Type A and Type B. These findings provide nuanced insights into the comparative stability and displacement characteristics of different tie rod configurations within the context of the parallel concrete panel structures.

5. Conclusions

This research involves modeling the PCP container with diagonal and horizontal tie-rod configurations to evaluate its performance. Based on the analysis of the modeling results, several significant conclusions were drawn regarding the structural configuration and integrity of the PCP container. Optimum tie rods configured horizontally (Type B) exhibit a reduced diameter requirement compared to diagonally configured ones (Type A). Nevertheless, Type B structures experience higher maximum moments, causing the concrete panels to be unable to withstand the loads acting on the structure and necessitating thicker concrete panels to ensure stability and load-bearing capacity. Concrete panels without horizontal tie rods cannot support the structure's weight. Therefore, integrating the dimensions of diagonal and horizontal tie rods, with diagonal tie rods being larger and horizontal tie rods being smaller, enhances the overall cost efficiency.

Meanwhile, the Plaxis 2D simulation analysis observed that Type A structures display stability with a safety factor of 1.35 and a total displacement of 0.2949 meters. In comparison, Type B structures exhibit stability with a safety factor of 1.32 and a total displacement of 0.2751 meters. Based on those results, both structures performed in a stable condition. It also suggests that the soil has sufficient strength to support the applied loads without failure.

This research implies that it can be used as an alternative design for shoreline protection structures. It is more eco-friendly because it requires less concrete and natural materials for construction. The structural integrity evaluation shows a stable result for diagonal and horizontal tie-rod configurations. The long-term durability of the material, especially considering the potential corrosion of steel tie rods, requires careful attention in extended-use scenarios. In future research, it is essential to compare numerical analysis with physical testing or similar structures to validate the analysis.

References

1) V.P. Nikijuluw, "Coastal resources conservation in Indonesia: issues, policies, and future directions," *Sumatra J. Disaster, Geogr. Geogr. Educ.*, **1** (*1*) 15 (2017). doi:10.24036/sjdgge.v1i1.31.

2) S.M. Permana, J. Risandi, C.K. Tito, M. Ramdhan, A. Sufyan, T. Solihuddin, D. Purbani, D.G. Pryambodo, R. Hidayat, H. Rifai, and K.M. Lukman, "Predicting coastal inundation triggered by the oceanic forcing across Jakarta bay," *IOP Conf. Ser. Earth Environ. Sci.*, **1109** (*1*) (2022). doi:10.1088/1755-1315/1109/1/012005.

3) Y. Prasetyo, N. Bashit, B. Sasmito, and W. Setianingsih, "Impact of land subsidence and sea level rise influence shoreline change in the coastal area of Demak," *IOP Conf. Ser. Earth Environ. Sci.*, **280** (*1*) (2019). doi:10.1088/1755-1315/280/1/012006.

4) H.Z. Abidin, H. Andreas, I. Gumilar, T.P. Sidiq, D. Pradipta, and B.D. Yuwono, "On the disaster risk reduction of land subsidence in Indonesia's northern coastal areas of Java," *EGU Gen. Assem.*, (*May*) 5194 (2022). doi:10.13140/RG.2.2.34300.00646.

5) P. Taneja, G. van R. van der Kloot, and M. van Koningsveld, "Sustainability performance of port infrastructure—a case study of a quay wall," *Sustain.*, **13** (*21*) 1–13 (2021). doi:10.3390/su132111932.

6) J. Wang, and E. Banzhaf, "Towards a better understanding of green infrastructure: a critical review," *Ecol. Indic.*, **85** (*December 2017*) 758–772 (2018). doi:10.1016/j.ecolind.2017.09.018.

7) V. Chávez, D. Lithgow, M. Losada, and R. Silva-Casarin, "Coastal green infrastructure to mitigate coastal squeeze," *J. Infrastruct. Preserv. Resil.*, **2** (*1*) 1–12 (2021). doi:10.1186/s43065-021-00026-1.

8) M.A. Benedict, and E.T. McMahon, "Smart conservation for the 21st century.," *Renew. Resour. J.*, **20** 12–17 (2002).

9) M. Yılmaz, and A. Bakış, "Sustainability in construction sector," *Procedia - Soc. Behav. Sci.*, **195** 2253–2262 (2015). doi:10.1016/j.sbspro.2015.06.312.

10) K. Sadeghi, and M. Almuhisen, "Concrete caisson breakwaters: an overview on design and construction," *Asian J. Nat. Appl. Sci.*, **6** (*4*) 100–106 (2017). www.ajsc.

11) US Army Corps Of Engineer, "Coastal Engineering Manual," Washington, DC, 2011.

12) J.A. Malik, and S. Marathe, "Ecological and health effects of building materials," *Ecol. Heal. Eff. Build. Mater.*, (*August*) 1–609 (2021). doi:10.1007/978-3-030-76073-1.

13) J.D. Sørensen, and H.F. Burcharth, "Reliability

analysis of geotechnical failure modes for vertical wall breakwaters," *Comput. Geotech.*, **26** (*3–4*) 225–245 (2000). doi:10.1016/S0266-352X(99)00040-3.

14) A.H. Dewi, Y. Lastiasih, and H. Wahyudi, "Perencanaan perbaikan tanah dan perkuatan tanggul lepas pantai teluk jakarta," *J. Tek. ITS*, **8** (*2*) (2020). doi:10.12962/j23373539.v8i2.48493.

15) PT. Jaya Wadah Lestari, "SUPW jwl panel," (n.d.). https://www.supwjwlpanel.com/ (accessed February 16, 2024).

16) D.I. Mazni, A. Hakam, J. Tanjung, F.A. Ismail, and Yossyafra, "Failure plane on precast block retaining wall," *Civ. Environ. Eng.*, **19** (*1*) 86–94 (2023). doi:10.2478/cee-2023-0008.

17) R. Berg, B. Christopher, and N. Samtani, "Design and construction of mechanically stabilized earth walls and reinforced soil slopes–volume i," *Fed. High W. Adm.*, **I** (*November*) (2009).

18) V. Elias, and B.R. Christopher, "Mechanically stabilized earth walls and reinforced soil slopes design and construction guidelines," in: FHWA-SA-96, Federal Highway Administration, Washington, D.C., 1997: p. 371.

19) S. Kim, D.E. Lee, Y. Kim, and S. Kim, "Development and application of precast concrete double wall system to improve productivity of retaining wall construction," *Sustain.*, **12** (*8*) (2020). doi:10.3390/SU12083454.

20) A.M. Hulagabali, C.H. Solanki, G.R. Dodagoudar, and Anitha, "Finite element analysis of segmental precast concrete panel reinforced earth retaining wall," *Jordan J. Civ. Eng.*, **17** (*4*) 582–597 (2023). doi:10.14525/JJCE.v17i4.03.

21) V.B. Chauhan, A. Srivastava, S. Jaiswal, and S. Keawsawasvong, "Behavior of back-to-back mse walls: interaction analysis using finite element modeling," *Transp. Infrastruct. Geotechnol.*, **10** (*5*) 888–912 (2023). doi:10.1007/s40515-022-00248-0.

22) Badan Standarisasi Nasional, "SNI 6880:2016 Spesifikasi Beton Struktural," BSN, Jakarta, 2016.

23) CSI Manual, "SAP2000 Integrated Solution for Structural Analysis and Design," Computers & Structures, Inc., Berkeley, California, USA, 2016.

24) Bentley, "PLAXIS 2D-Reference Manual," V20.02, 2020.

25) K. Gowda, "Analysis of counterfort retaining wall with and without pressure relief shelf using soft computing technique science insights : an international journal issn 2277 – 3835 original article analysis of counterfort retaining wall with and without pressure rel," (*January*) (2017).

26) P. Yadav, D.K. Singh, P.P. Dahale, and A.H. Padade, "Analysis of retaining wall in static and seismic condition with inclusion of geofoam using plaxis 2d," *Lect. Notes Civ. Eng.*, **86** (*December*) 223–240 (2021). doi:10.1007/978-981-15-6233-4_16.

27) Y. Goda, and H. Takagi, "Reliability design method of caisson breakwaters with optimal wave heights," *Coast. Eng. J.*, **42** (*4*) 357–387 (2000). doi:10.1016/S0578-5634(00)00018-3.

28) OCDI, "Technical Standards and Commentaries for Port and Harbour Facilities in Japan," The Overseas Coastal Area Development Institute, Tokyo, Japan, 2020.

29) Y. Goda, "The design of upright breakwater," *Proc. Short Course Des. Reliab. Coast. Struct.*, 547–566 (1993).

30) S. Takahashi, "Design of Vertical," Revised Ve, Port and Airport Research Institute, JAPAN, 2002.

31) B. M. Das, and S. Nagaratnam, "Principles of Foundation Engineering," SI Edition, Cengage Learning, Inc., USA, 2019.

32) Badan Standarisasi Indonesia, "SNI 1726:2019 Tata cara perencanaan ketahanan gempa untuk struktur bangunan gedung dan nongedung," BSN, Jakarta, 2020.

33) Badan Standardisasi Indonesia, "SNI 1727:2020 Beban desain minimum dan Kriteria terkait untuk bangunan gedung dan struktur lain," BSN, Jakarta, 2020.

34) Badan Standardisasi Nasional, "SNI 8460:2017 Persyaratan Perancangan Geoteknik," BSN, Jakarta, 2017.

35) R. Damanik, E. Gunawan, S. Widiyantoro, P. Supendi, F.W. Atmaja, Ardianto, Y.M. Husni, Zulfakriza, and D.P. Sahara, "New assessment of the probabilistic seismic hazard analysis for the greater Jakarta area, Indonesia," *Geomatics, Nat. Hazards Risk*, **14** (*1*) (2023). doi:10.1080/19475705.2023.2202805.

36) R. B. J. Brinkgreve, "Plaxis finite element code for soil and rock analyses, Version 8," Balkema, Rotterdam, 2002.

37) S.H. Lajevardi, K. Malekmohammadi, and D. Dias, "Numerical study of the behavior of back-to-back mechanically stabilized earth walls," *Geotechnics*, **1** (*1*) 18–37 (2021). doi:10.3390/geotechnics1010002.